Supporting Information

Structural Regulation of Zinc-Porphyrin Frameworks via the Auxiliary Nitrogen-containing Ligands towards the Selective Adsorption of Cationic Dyes

Xiaoning Wang,[a] Jiangli Li,[a] Yumeng Zhao,[a] Jiandong Pang,[b] Bao Li[a],, Tian-Le Zhang[a] and Hong-Cai Zhou[b],**

[a] Key laboratory of Material Chemistry for Energy Conversion and Storage, School of Chemistry and Chemical Engineering, Huazhong University of Science and Technology, Wuhan, Hubei, 430074, P. R. China.

[b] Department of Chemistry, Texas A&M University, College Station, Texas 77843-3255, United States.

* Corresponding Author
*E-mail: libao@hust.edu.cn (B. L.).
*E-mail: zhou@chem.tamu.edu (H.-C. Z.).

Experimental Section

Materials and General Methods

The organic ligand H_4TCPP was synthesized according to a literature method[1,2] and all of the starting reagents for the syntheses were commercially available and were used as received. Elemental analyses (C, H and N) were performed on a Perkin-Elmer 2400 analyzer. The IR spectra were recorded with KBr pellets on a Nicolet Avatar-360 spectrometer in the 4000–400 cm^{-1} region. Thermogravimetric analysis (TGA) was carried out with a Perkin-Elmer TG-7 analyzer heated from room temperature to 800 °C, using a heating rate of 10 °C min^{-1} under air. Powder X-ray diffraction (PXRD) patterns were measured on the Rigaku model Ultima IV diffractometer with Cu-Ka radiation. Ultraviolet-visible (UV-vis) adsorption spectra were recorded at room temperature on UV-2550 spectrophotometer.

Synthesis of meso-tetra (4-carboxyphenyl) porphyrin (H_6TCPP)

The preparation of H_6TCPP was carried out following the previously described procedure with slightly modifications. Briefly, in a 1 L round-bottom flask equipped with magnetic stirrer, 25 g of 4-formylbenzoic acid (0.16 mol) was added to 600 mL of propionic acid. The mixture was stirred and heated to 70 °C at which temperature the aldehyde fully dissolved. Then a propionic acid solution (10 mL) of freshly distilled pyrrole (11.2 g, 0.17 mol) was added dropwise to the reaction mixture. The resultant dark mixture was refluxed with continued stirring for 4 h. The solid product was then separated by filtration and was washed several times with dichloromethane (DCM) followed by a small amount of distilled water in order to remove unreacted propionic acid and impurities. After that, the resulting purple solid was collected and dried overnight (about 50% yield). ^{1}H-NMR (400 MHz, DMSO-d^6): δ 8.86 (8H, s, β-H), 8.36 (16H, dd, o+m ArH), 2.93 (2H, s, NH). ^{13}C-NMR (101 MHz, DMSO-d^6): δ 167.5, 145.3, 134.4, 130.5, 127.8, 119.2.

Synthetic routes of 1-3
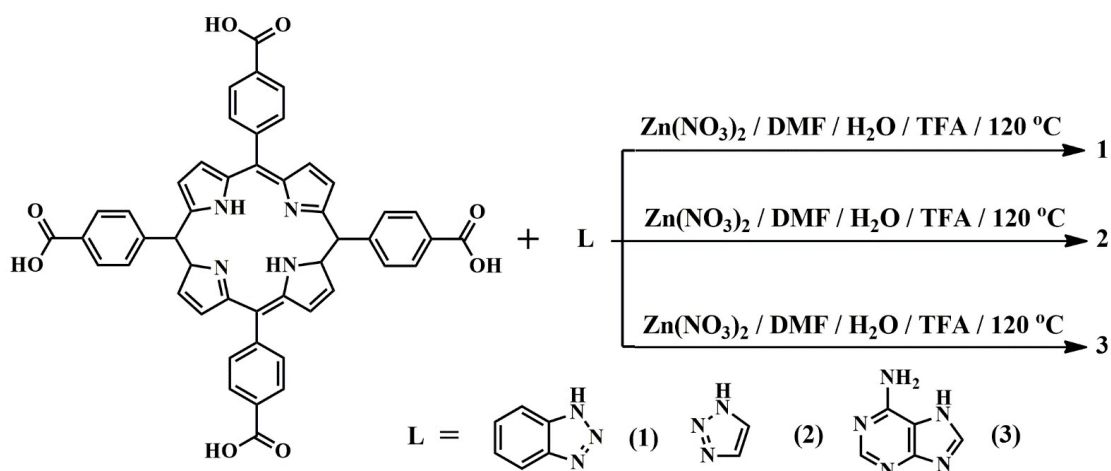
Scheme S1. Synthetic routes of **1**, **2**, and **3** under solvothermal condition.

Synthesis of Compound 1

A mixture of Zn(Ac)$_2$·2H$_2$O (5 mg, 0.023 mmol), H$_6$TCPP (3 mg, 0.004 mmol), benzotriazole (2 mg, 0.017 mmol), DMF (2 mL), H$_2$O (0.5 mL) and trifluoroacetic acid (5 drops) was sealed in a 5 mL glass vial, which was heated at 120 °C for 72 h in an oven, purplish block crystals were obtained. The yield was 30% for **1** (based on H$_6$TCPP ligand). IR (KBr, cm^{-1}): 3438 (s, br), 2920 (w), 1649 (vs), 1541 (w), 1386 (vs), 1317 (m), 1179 (w), 1082 (m), 994 (s), 838 (m), 769 (s), 710 (w), 661 (w). Elemental analysis calcd (%) for **1** (C$_{54}$H$_{28}$N$_7$O$_8$Zn$_3$): C, 59.01; H, 2.57; N, 8.92; found: C, 59.53, H, 3.96, N, 9.26.

Synthesis of Compound 2

A mixture of Zn(Ac)$_2$·2H$_2$O (5 mg, 0.023 mmol), H$_6$TCPP (7 mg, 0.009 mmol), 1H-1,2,3-triazole (3 mg, 0.043 mmol), DMF (2 mL), H$_2$O (0.5 mL) and trifluoroacetic acid (5 drops) was sealed in a 5 mL glass vial, which was heated at 120 °C for 72 h in an oven, purplish block crystals were obtained. The yield was 30% for **2** (based on H$_6$TCPP ligand). IR (KBr, cm^{-1}): 3438 (m, br), 2920 (w), 1610 (vs), 1531 (m), 1386 (vs), 1199 (w), 1102 (m), 995 (m), 779 (s), 721 (m), 583 (w). Elemental analysis calcd (%) for **2** (C$_{168}$H$_{120}$N$_{48}$O$_{36}$Zn$_{13}$): C, 47.62; H, 2.85; N, 15.87; found: C, 48.23, H, 3.49, N, 16.04.

Synthesis of Compound 3

A mixture of Zn(Ac)$_2$·2H$_2$O (10 mg, 0.046 mmol), H$_6$TCPP (14 mg, 0.018 mmol), adenine (6 mg, 0.044 mmol), DMF (2 mL), H$_2$O (0.5 mL) and trifluoroacetic acid (10

drops) was sealed in a 5 mL glass vial, which was heated at 120 °C for 72 h in an oven, purplish block crystals were obtained. The yield was 60% for **3** (based on H_6TCPP ligand). IR (KBr, cm^{-1}): 3418 (m, br), 3203 (w), 2929 (w), 1659 (vs), 1601(vs), 1551 (m), 1385 (vs), 1209 (m), 1092 (m), 994 (m), 847 (m), 769 (s), 662 (m). Elemental analysis calcd (%) for **3** ($C_{154}H_{84}N_{22}O_{28}Zn_9$): C, 56.41; H, 2.58; N, 9.40; found: C, 56.53, H, 3.09, N, 10.06.

Single Crystal X-ray Diffraction. The crystal data for **1** were collected on Va Bruker Venture using Cu-$K\alpha$ (= 1.54178 Å) radiation at 100 K. The structure of the **1-3** was solved by direct methods, and the non-hydrogen atoms were located from the trial structure and then refined anisotropically with SHELXTL using a full-matrix least squares procedure based on F^2 values.[3] All hydrogen atoms were generated geometrically and refined using a riding model. The contribution of the missing solvent molecule and other ionic residues to the diffraction patterns was removed from the reflection data by the SQUEEZE method as implemented in PLATON to afford a set of solvent free diffraction intensities.[4] CCDC 1848723-1848725 contain the supplementary crystallographic data for this paper. The data can be obtained free of charge at www.ccdc.cam.ac.uk/conts/retrieving.html or from the Cambridge Crystallographic Data Centre, 12, Union Road, Cambridge CB2 1EZ, UK. The details for structural analyses of the **1-3** were listed in Table S1 and Table S2-4.

Low Pressure Gas Sorption Measurements

Low-pressure N_2 adsorption measurements (up to 1 bar) were performed on Micromeritics ASAP 2020 M+C surface area and pore size analyzer. The as synthesized samples (200 mg) were soaked in acetone for two days, during which the solvent was refreshed six times and subsequently dried under dynamic vacuum at room temperature. Helium was used for the estimation of the dead volume, assuming that it is not adsorbed at any of the studied temperatures. To provide high accuracy and precision in determining P/P_0, the saturation pressure P_0 was measured throughout the N_2 analyses by means of a dedicated saturation pressure transducer, which allowed us to monitor the vapor pressure for each data point. A part of the N_2 sorption isotherm in the P/P_0 range 0.01–0.1 was fitted to the BET equation to estimate the

BET surface area and the Langmuir surface area calculation was performed using all data points. The pore size distribution (PSD) was obtained from the DFT model in the Micromeritics ASAP2020 software package (assuming slit pore geometry) based on the N_2 sorption at 77 K.

Dyes adsorption experiments

Dye-uptake analyses were executed by soaking the fresh samples of **1-3** (10 mg) in DMF solutions containing different kinds of dyes (5 mL, 2.5×10^{-5} mmol·L^{-1}), respectively, and the progress was monitored by UV-vis spectroscopy at various time intervals. The adsorption degree had been calculated based on UV/vis spectroscopy testing results. The amounts of absorbed dyes at time q_t and adsorption kinetics constant were calculated as follows:[5]

$$q_t = (C_0 - C)\frac{V}{m} \qquad (1)$$

$$\ln(C_0/C) = k_1 t \qquad (2)$$

$$\frac{t}{q_t} = \frac{1}{k_2 q_e^2} + \frac{t}{q_e} \qquad (3)$$

in which C_0 and C are the concentrations of dyes at initial and time, respectively (in mg L^{-1}). V is the volume of the dye solutions (in L) and m is the mass of MOF adsorbents (in g). k_1 and k_2 are the pseudo-first-order rate constant (in min^{-1}) and pseudo-second-order rate constant (in g mg^{-1} min^{-1}), respectively. k_1 and k_2 can be obtained from the fitted plots of $\ln(C_0/C)$ vs. t and t/q_t vs. t, respectively.
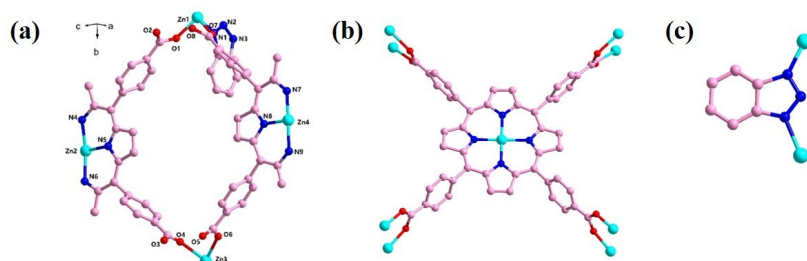
The Structure of 1-3

Figure. S1 The asymmetrical unit of **1** (a); the coordination modes of TCPP ligand (b) and benzotriazole ligand in **1**(c).
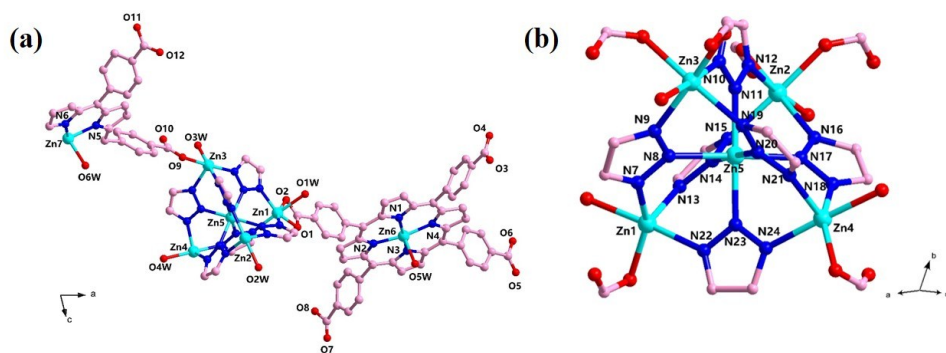
Figure. S2 The asymmetrical unit of **2** (a); the [Zn₅(tra)₆]⁴⁺ clusters of **2** (b).
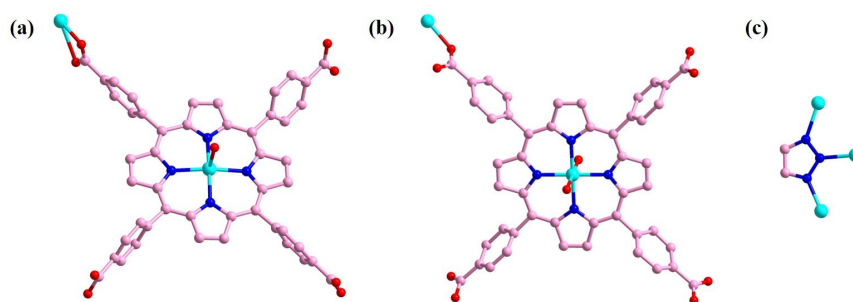

Figure. S3 The coordination modes of TCPP ligand (a, b)
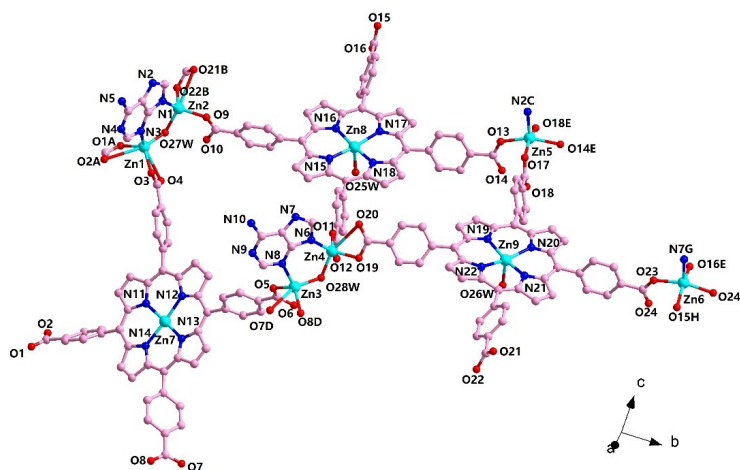
and 1,2,3- triazole ligand (c) in **2**.

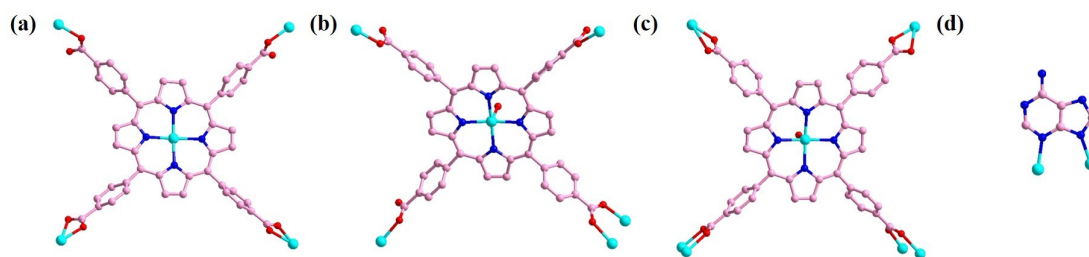**Figure. S4** The asymmetrical unit of **3**.

Figure. S5 The coordination modes of TCPP ligand (a-c) and adenine ligand (d) in **3**.

Table S1. Crystal Data and Structure Refinement Details for **1-3**.

	1	2	3
Empirical formula	$C_{54} H_{28} N_7 O_8 Zn_3$	$C_{168} H_{120} N_{48} O_{36} Zn_{13}$	$C_{154} H_{84} N_{22} O_{28} Zn_9$
Formula weight	1098.94	4236.92	3278.76
Temperature/K	293(2)	293(2)	293(2)
Crystal system	orthorhombic	triclinic	triclinic
Space group	P n n m	P -1	P -1
a/Å	17.2954(7)	19.0940(16)	25.4598(13)
b/Å	33.2059(11)	24.290(2)	26.2974(14)
c/Å	33.2059(11)	24.738(2)	31.8554(17)
α/°	90	61.042(5)	90.284(3)
β/°	90	73.947(6)	92.982(3)
γ/°	90	82.746(6)	98.728(3)
Volume/Å^3	19070.5(12)	9647.0(16)	21050.7(19)
Z	2	1	2
ρ_{calc}g/cm^3	0.191	0.729	0.517
μ/mm^{-1}	0.287	1.205	0.787
Final R indexes [I>=2σ (I)]	R_1 = 0.1358/wR_2 = 0.3669	R_1 = 0.1128/wR_2 = 0.3020	R_1 = 0.0896/wR_2 = 0.2395
Final R indexes [all data]	R_1 = 0.1897/ wR_2 = 0.4073	R_1 = 0.1576/ wR_2 = 0.3253	R_1 = 0.1373/wR_2 = 0.2590

Table S2. Bond Lengths for **1**.

Atom	Atom	Length/Å	Atom	Atom	Length/Å
Zn1	O1	1.984(5)	Zn3	O2^3	1.992(5)
Zn1	N1	1.862(12)	Zn3	N3^4	2.087(11)
Zn1	Zn3^1	2.9478(18)	Zn3	O4	2.160(6)
Zn1	O3^1	2.086(5)	Zn3	O6	2.122(7)
Zn1	O5^1	2.053(10)	Zn3	O8^3	1.991(7)
Zn1	O7	1.846(7)	Zn3	N15^4	2.145(12)
Zn1	N14	1.857(12)	O2	Zn3^1	1.992(5)
O3	Zn1^3	2.086(5)	O8	Zn3^1	1.991(7)
O5	Zn1^3	2.053(10)	N3	Zn3^4	2.087(11)
Zn2	N4	2.068(7)	N15	Zn3^4	2.145(12)
Zn2	N5	2.078(5)	Zn4	N7	1.961(11)
Zn2	N5^2	2.078(5)	Zn4	N8^5	2.030(10)

Atom	Atom	Length/Å	Atom	Atom	Length/Å
Zn2	N6	2.095(7)	Zn4	N8	2.030(10)
Zn3	Zn1[3]	2.9478(18)	Zn4	N9	2.096(15)

Symmetry code for **1**: [1]1/2-X,-1/2+Y,1/2-Z; [2]+X,+Y,1-Z; [3]1/2-X,1/2+Y,1/2-Z; [4]1-X,1-Y,+Z; [5]+X,+Y,-Z

Table S3. Bond Lengths for **2**.

Atom	Atom	Length/Å	Atom	Atom	Length/Å
Zn1	N22	2.152(5)	Zn5	N11	2.115(5)
Zn1	N7	2.020(6)	Zn5	N23	2.161(5)
Zn1	O1	2.024(7)	Zn5	N8	2.190(6)
Zn1	N13	2.050(6)	Zn5	N17	2.180(5)
Zn1	O1W	2.266(5)	Zn5	N20	2.177(6)
Zn1	C1	2.533(10)	Zn5	N14	2.181(6)
Zn2	N16	2.132(5)	Zn6	N1	2.034(5)
Zn2	O6[2]	2.115(5)	Zn6	N2	2.049(6)
Zn2	O2W	2.165(5)	Zn6	N3	2.028(5)
Zn2	O12[3]	2.082(5)	Zn6	N4	2.054(6)
Zn2	N15	2.131(6)	Zn6	O5W	2.326(9)
Zn2	N12	2.186(7)	Zn7	N5	2.035(6)
Zn3	O4[1]	2.121(4)	Zn7	N5[5]	2.035(6)
Zn3	N9	2.136(5)	Zn7	N6[5]	2.026(6)
Zn3	O3W	2.185(6)	Zn7	N6	2.026(6)
Zn3	O9	2.088(5)	Zn7	O6W	2.393(14)
Zn3	N10	2.116(7)	Zn7	O6W[5]	2.393(14)
Zn3	N19	2.135(5)	O6	Zn2[6]	2.115(5)
Zn4	N24	2.137(6)	O12	Zn2[3]	2.082(5)
Zn4	N18	2.086(6)	O4	Zn3[1]	2.121(4)
Zn4	N21	2.059(6)	C44	Zn4[4]	2.485(11)
Zn4	O4W	2.200(5)	O7	Zn4[4]	2.105(8)
Zn4	O8[4]	2. 364 (8)	O8	Zn4[4]	2.364(8)
Zn4	O74	2.105(8)			
Zn4	C44[4]	2.485(12)			

Symmetry code for **2**: [1]2-X,1-Y,2-Z; [2]-1+X,1+Y,+Z; [3]1-X,2-Y,2-Z; [4]1-X,-Y,3-Z; [5]-X,2-Y,2-Z; [6]1+X,-1+Y,+Z

Table S4. Bond Lengths for **3**.

Atom	Atom	Length/Å	Atom	Atom	Length/Å
Zn1	O1[1]	1.928(4)	O14	Zn5[5]	2.058(3)
Zn1	O3	1.930(5)	O18	Zn5[5]	2.022(3)
Zn1	N3	2.035(5)	Zn6	Zn6[6]	2.9977(14)
Zn1	O27W	1.941(3)	Zn6	N7[7]	2.009(5)
O1	Zn1[1]	1.928(4)	Zn6	O15[8]	2.044(3)
Zn2	O9	1.954(3)	Zn6	O16[5]	2.044(3)
Zn2	O22[2]	1.976(3)	Zn6	O23	2.037(3)
Zn2	O27W	1.982(3)	Zn6	O24[6]	2.057(3)
N1	Zn2	2.010(4)	O15	Zn6[2]	2.045(3)
N2	Zn5[3]	2.006(4)	O16	Zn6[5]	2.044(3)
O22	Zn2[8]	1.976(3)	O24	Zn6[6]	2.057(3)
Zn3	O5	1.904(6)	N7	Zn6[7]	2.009(5)
Zn3	O8[4]	1.967(4)	Zn7	N11	2.013(5)
Zn3	N8	2.059(5)	Zn7	N12	2.052(5)
Zn3	O28W	1.921(3)	Zn7	N13	2.060(5)
O8	Zn3[4]	1.967(4)	Zn7	N14	2.064(5)
Zn4	N6	1.996(4)	Zn8	N15	2.039(4)
Zn4	O11	1.952(3)	Zn8	N16	2.038(3)
Zn4	O19	1.955(3)	Zn8	N17	2.071(4)
Zn4	O28W	1.993(3)	Zn8	N18	2.044(3)
Zn5	N2[3]	2.006(4)	Zn8	O25W	2.326(5)
Zn5	Zn5[5]	2.9636(14)	Zn9	N19	2.075(3)
Zn5	O13	2.007(4)	Zn9	N20	2.060(3)
Zn5	O14[5]	2.058(3)	Zn9	N21	2.063(3)
Zn5	O17	2.049(3)	Zn9	N22	2.054(4)
Zn5	O18[5]	2.022(3)	Zn9	O26W	2.168(4)

Symmetry code for **3**: [1]1-X,1-Y,1-Z; [2]-1+X,-1+Y,+Z; [3]1-X,2-Y,2-Z; [4]2-X,2-Y,1-Z; [5]1-X,3-Y,2-Z; [6]2-X,4-Y,2-Z; [7]2-X,3-Y,2-Z; [8]1+X,1+Y,+Z
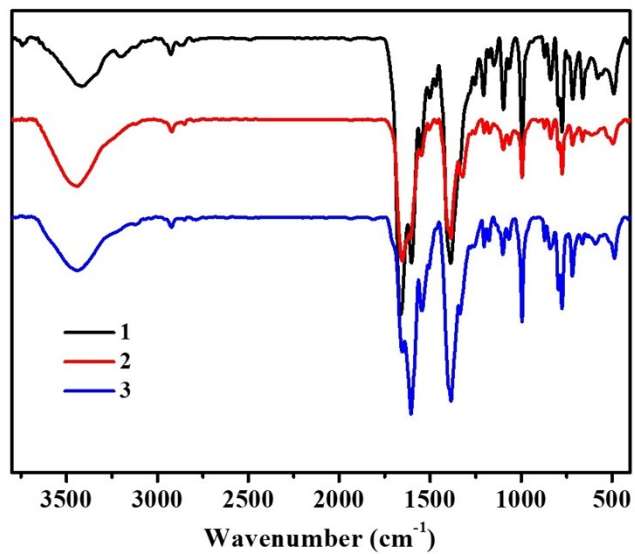
Figure S6. IR spectra of **1** (black), **2** (red) and **3** (blue).
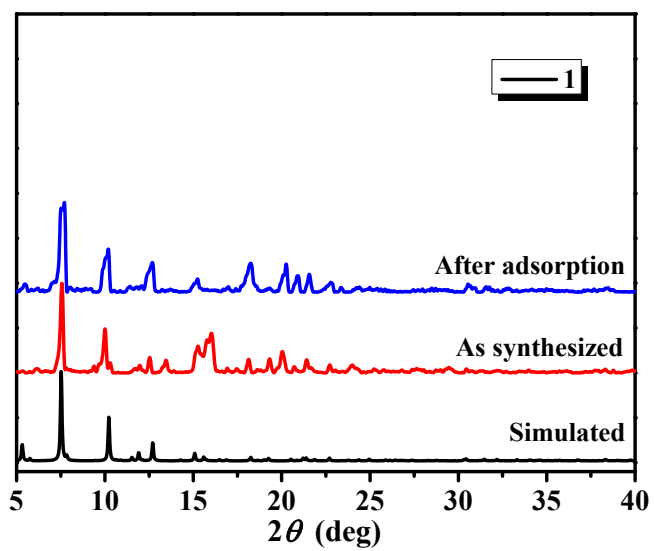
Figure S7. PXRD patterns of **1**.
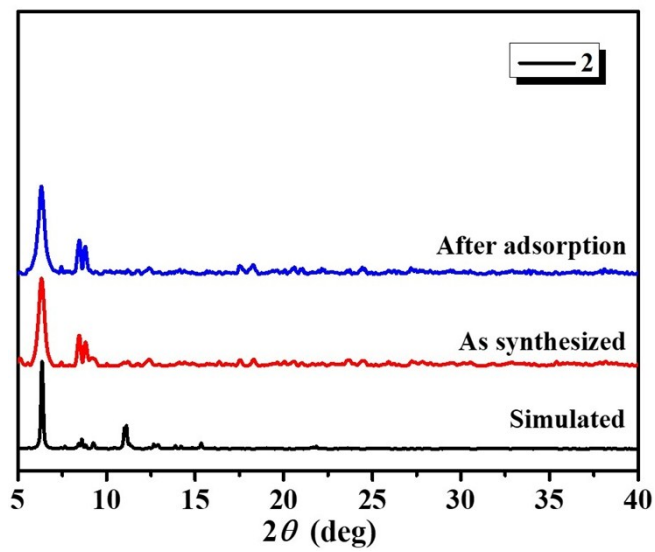
Figure S8. PXRD patterns of **2**.
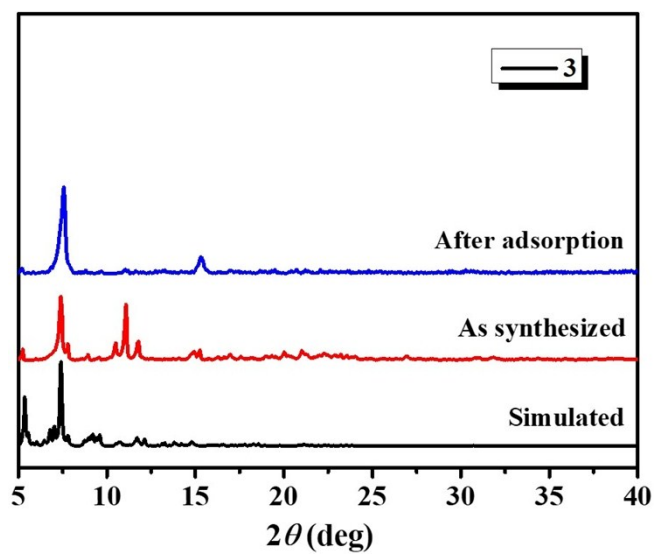
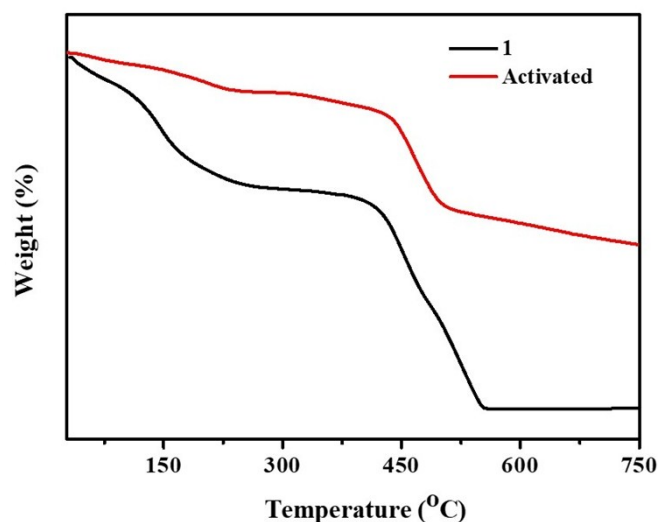**Figure S9.** PXRD patterns of **3**.

Figure S10. TGA curves of **1** under air atmosphere. The thermogravimetry curve of **1** showed a sharp weight loss of 31.4 % from 30 to 300 °C, which may be regarded as the escape of coordinated water and lattice DMF molecules. The structure can stable up to 400 °C, and then the rapid weight loss could be attributed to the collapse of the framework of **1**.
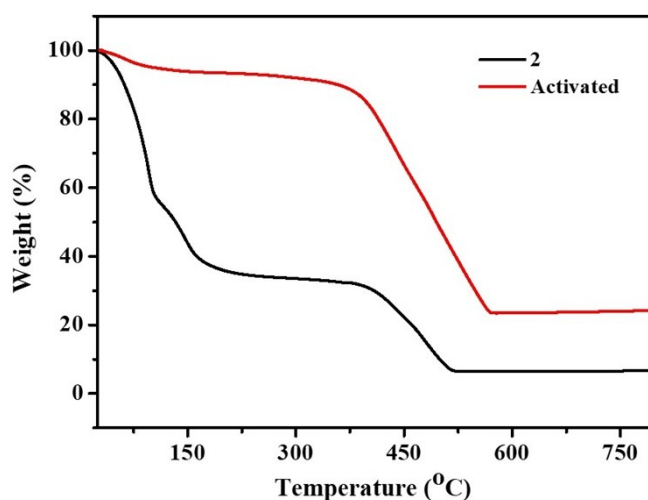
Figure S11. TGA curves of **2** under air atmosphere. In the case of **2**, the observed weight loss of 64.4% in the temperature range of 30 to 235 °C may be due to the loss of DMF and water molecules. A flat region in the temperature range 235–400 °C indicates that the framework may be stable until 400 °C. A steady weight loss was observed above 400 °C suggesting a collapse of the framework.
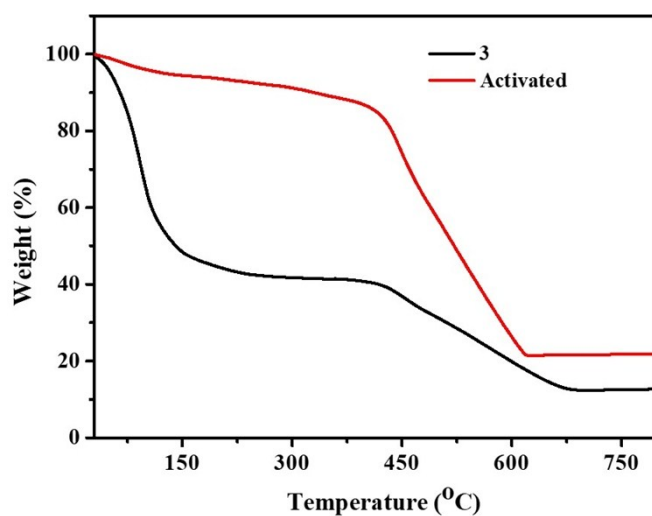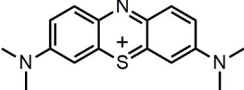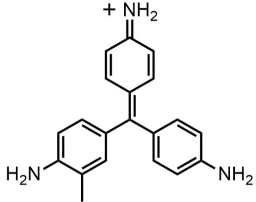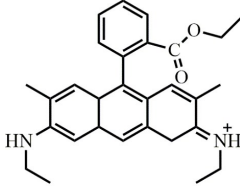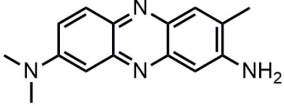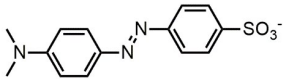
Figure S12. TGA curves of **3** under air atmosphere. Complex **3** exhibits similar behavior to that of complexes **1-2** in the initial TGA studies. A weight loss of approximately 57.6% in the temperature range 30–240 °C corresponds to the loss of DMA and water molecules. Then a flat region in the temperature range 240–400 °C demonstrates that the structure can stable up to 400 °C. A more significant weight loss above the 400 °C corresponds to the collapse of the framework.

Table S5. Molecular dimensions of relative dyes with different charges.[6-8]

Dyes	Charge	Dimensions (Å)
 Methylene Blue (MB$^+$)	+1	1.8×5.5×14.2
 Basic Violet 14 (BV14$^+$)	+1	2.9×11.0×12.5

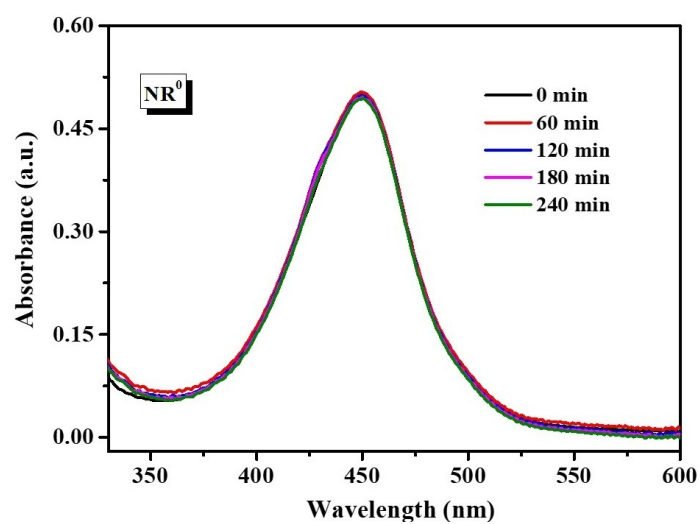|		
Rhodamine 6G (Rh6G⁺)	+1	10.9×15.7×15.8
Neutral Red (NR)	0	2.3×6.4×12.6
Methylene Orange (MO⁻)	-1	4.5×6.0×14.8

Figure S13. UV-vis spectra of DMF solutions of neutral red (NR^0) in the presence of complex **3** with time.
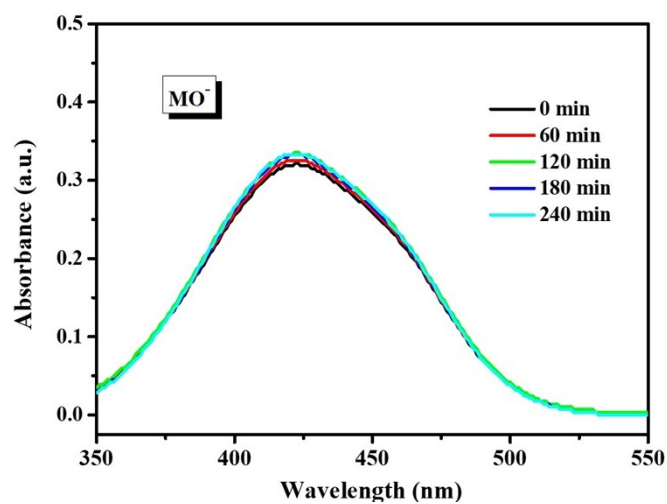
Figure S14. UV-vis spectra of DMF solutions of methyl orange (MO⁻) in the presence
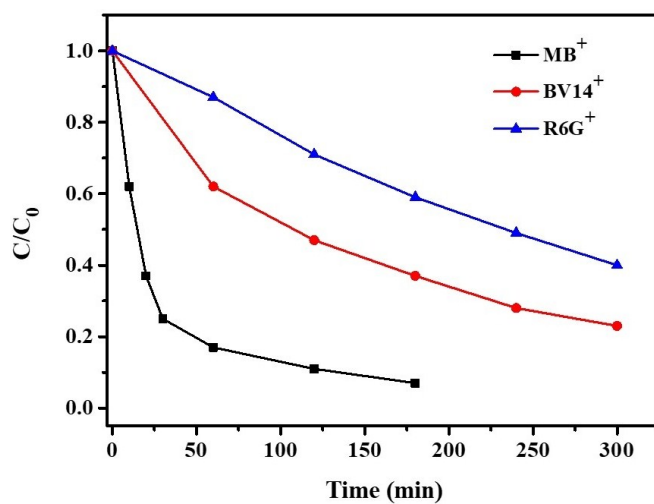
of complex **3** with time.

Figure S15. The concentration changes of dyes with different sizes and same charge
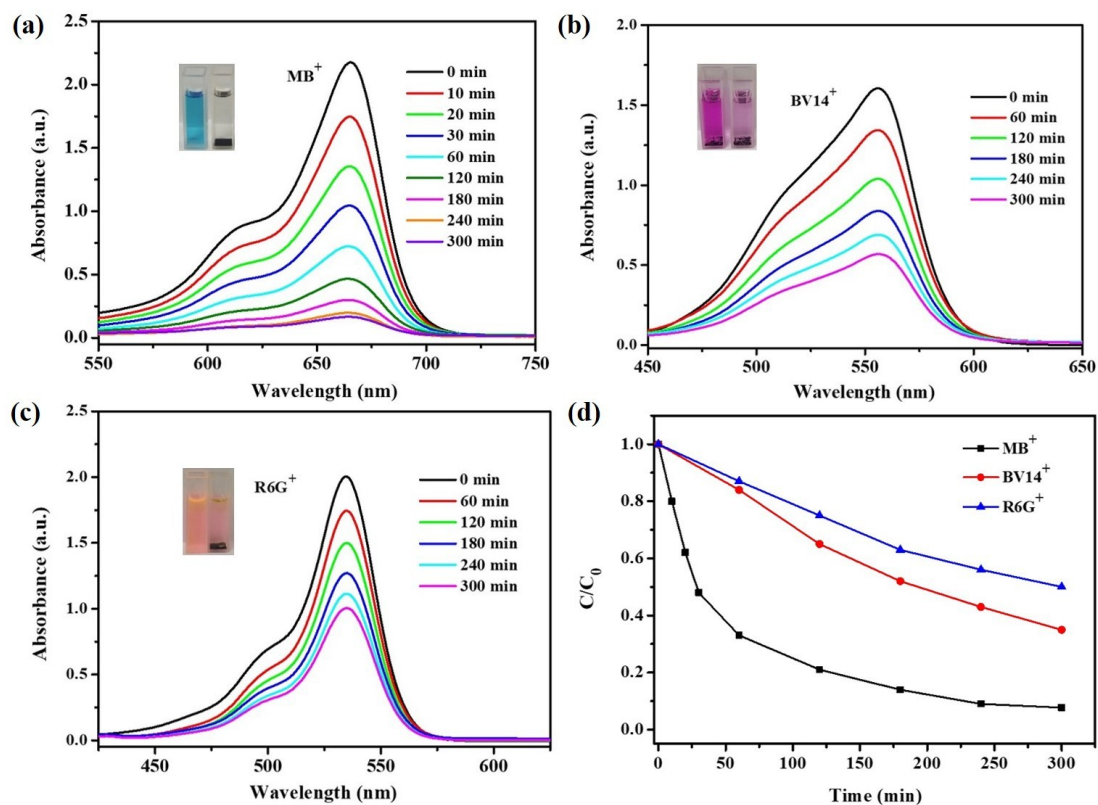
in the presence of complex **3** with time.

Figure S16. UV-vis spectra of DMF solutions of methylene blue (MB$^+$) (a), basic violet 14 (BV14$^+$) (b), and rhodamine 6G (Rh6G$^+$) (c) in the presence of complex **2** at different times. The inset images display the change in colors before and after the dye adsorption by complex **2**. (d) The concentration changes of dyes with different sizes and same charge in solution along with adsorption time.
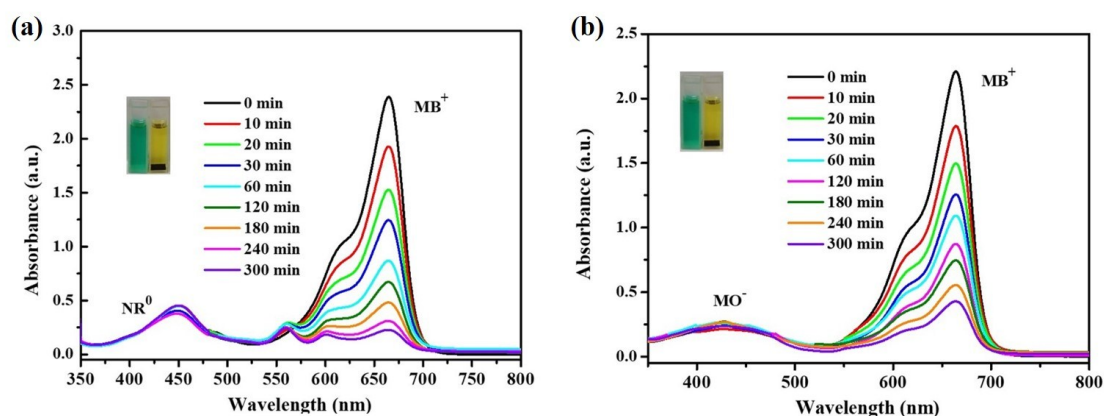

Figure S17. UV-Vis absorption spectra of equimolar MB$^+$ & NR^0 (a) and MB$^+$ & MO$^-$ (b) in the presence of complex **2** at different times. The inset images display the change in colors before and after the dye adsorption by complex **2**.
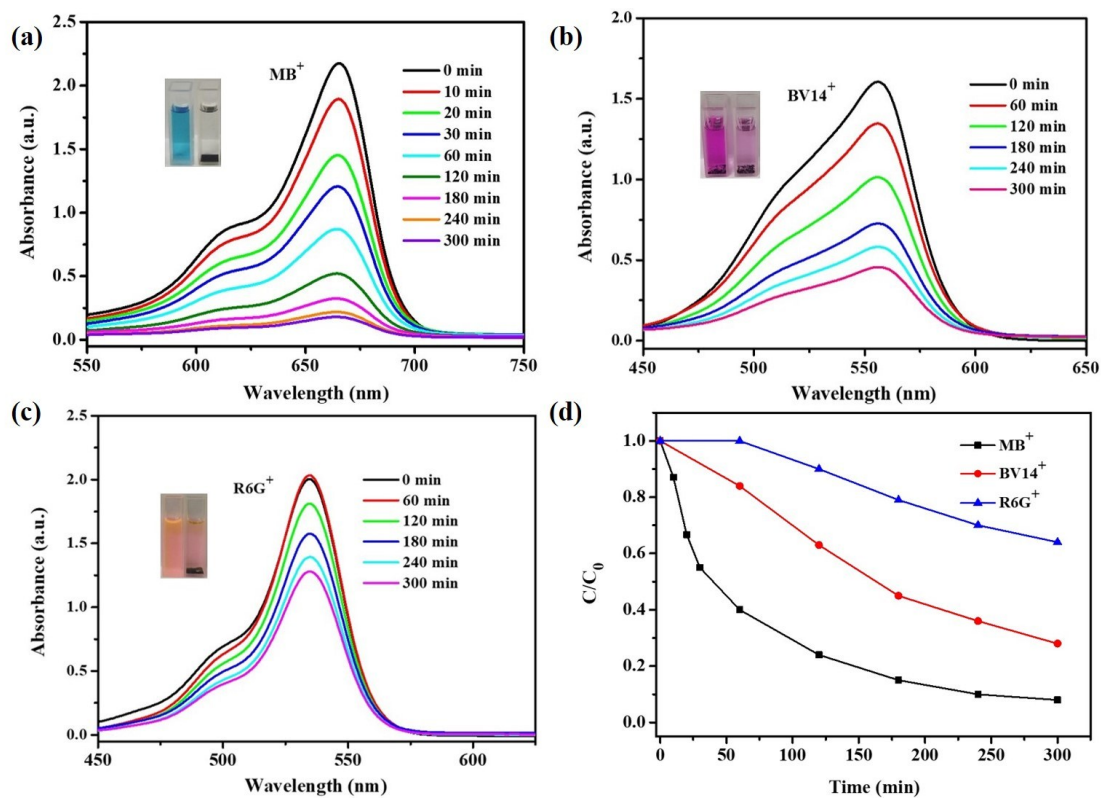
Figure S18. UV-vis spectra of DMF solutions of methylene blue (MB[+]) (a), basic violet 14 (BV14^{+}) (b), and rhodamine 6G (Rh6G^{+}) (c) in the presence of complex **3** at different times. The inset images display the change in colors before and after the dye adsorption by complex **3**. (d) The concentration changes of dyes with different sizes and same charge in solution along with adsorption time.
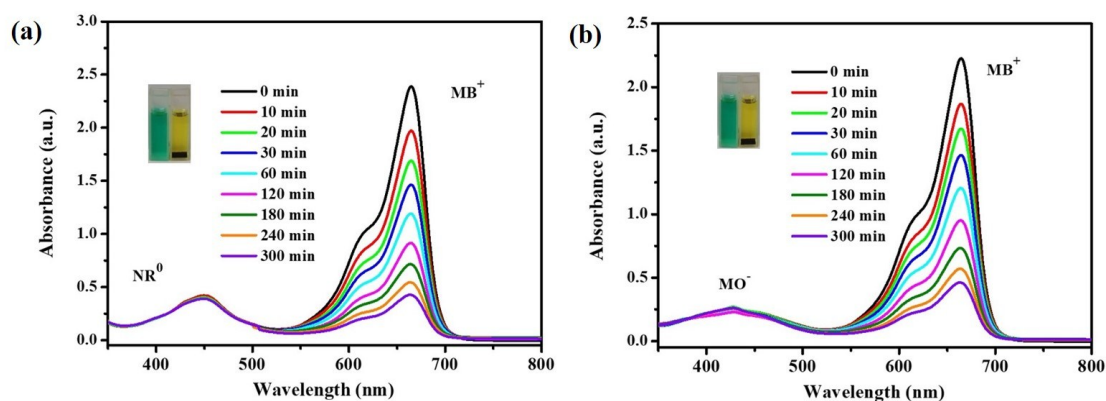

Figure S19. UV-Vis absorption spectra of equimolar MB[+] & NR[0] (a) and MB[+] & MO[-] (b) in the presence of complex **3** at different times. The inset images display the change in colors before and after the dye adsorption by complex **3**.
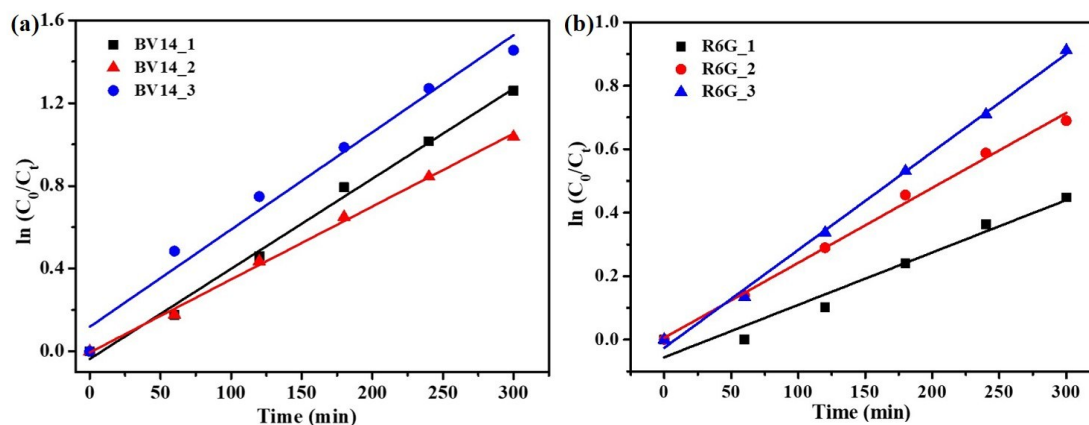
Figure S20. The corresponding kinetic data fitting of BV14 (a),

R6G (b) adsorption over **1-3** using the pseudo-first-order kinetics model.

Table S6. Kinetic parameters of MB^+, $BV14^+$ and $R6G^+$ adsorbed into **1-3**.

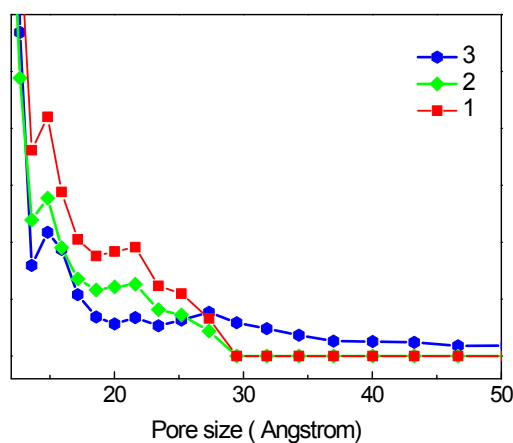| Samples	First order k_1 (min^{-1})				Second order k_2 (g mg^{-1} min^{-1})	
	$BV14^+$	R^2	$R6G^+$	R^2	MB^+	R^2
1	4.4×10^{-3}	0.9931	1.7×10^{-3}	0.9495	5.3×10^{-3}	0.9711
2	3.5×10^{-3}	0.9972	2.4×10^{-3}	0.9945	8.1×10^{-3}	0.9882
3	4.7×10^{-3}	0.9719	3.1×10^{-3}	0.9968	2.54×10^{-2}	0.9942

Figure S21. Pore size distribution of three zinc MOFscalculated from N_2 sorption isotherms by density functional theory (DFT) method.

References

(1) D. Daly, A. Al-Sabi, G. K. Kinsella, K. Nolan and J. O. Dolly, *Chem. Commun.,*
2015, **51**, 1066.

(2) A. K. Yetisen, M. M. Qasim, S. Nosheen, T. D. Wilkinson and C. R. Lowe, *J.*

Mater. Chem. C, 2014, **2**, 3569.

(3) O. V. Dolomanov, L. J. Bourhis, R. J. Gildea, J. A. K. Howard, H. Puschmann, *J. Appl. Cryst.,* 2009, **42**, 339.

(4) A. L. Spek, *J. Appl. Cryst.,* 2003, **36**, 7.

(5) Q. Li, D. -X. Xue, Y.-F. Zhang, Z.-H. Zhang, Z. W. Gao and J. F. Bai, *J. Mater. Chem. A,* 2017, **5**, 14182.

(6) S. Yao, T. Xu, N. Zhao, L. Zhang, Q. Huo and Y. Liu, *Dalton Trans.,* 2017, **46**, 3332.

(7) Y, Song, R.-Q. Fan, K. Xing, X. Du, T. Su, P. Wang and Y.-L. Yang, *Cryst. Growth Des.,* 2017, **17**, 2549.

(8) D. M. Chen, J. Y. Tian, Z. W. Wang, C. S. Liu, M. Chen and M. Du, *Chem. Commun.,* 2017, **53**, 10668.